

EPR study of the dynamic spin susceptibility in heavily doped $\text{YBa}_2\text{Cu}_3\text{O}_{6+\delta}$

J. Sichelschmidt, B. Elschner, Alois Loidl, B. I. Kochelaev

Angaben zur Veröffentlichung / Publication details:

Sichelschmidt, J., B. Elschner, Alois Loidl, and B. I. Kochelaev. 1995. "EPR study of the dynamic spin susceptibility in heavily doped $\text{YBa}_2\text{Cu}_3\text{O}_{6+\delta}$." *Physical Review B* 51 (14): 9199–9207. <https://doi.org/10.1103/physrevb.51.9199>.

Nutzungsbedingungen / Terms of use:

licgercopyright

Dieses Dokument wird unter folgenden Bedingungen zur Verfügung gestellt: / This document is made available under these conditions:

Deutsches Urheberrecht

Weitere Informationen finden Sie unter: / For more information see:

<https://www.uni-augsburg.de/de/organisation/bibliothek/publizieren-zitieren-archivieren/publiz/>



EPR study of the dynamic spin susceptibility in heavily doped $\text{YBa}_2\text{Cu}_3\text{O}_{6+\delta}$

J. Sichelschmidt, B. Elschner, and A. Loidl*

Institut für Festkörperphysik, Technische Hochschule Darmstadt, 64289 Darmstadt, Germany

B. I. Kochelaev

Department of Physics, Kazan State University, Kazan, 420008, Russia

(Received 2 May 1994)

Electron paramagnetic resonance (EPR) studies on single crystals of $\text{YBa}_2\text{Cu}_3\text{O}_{6+\delta}$ were performed in a wide range of oxygen concentration δ . Intrinsic EPR signals due to the existence of paramagnetic chain fragments could be detected only in a limited δ range ($0.7 \leq \delta \leq 0.9$). The linewidth of the signal passes through a minimum near 105 K and broadens exponentially for further decreasing temperatures. This behavior manifests the opening of a pseudogap in the dynamic spin susceptibility of the CuO_2 planes. At higher temperatures the linewidth follows a Korringa behavior. The g values reveal axial symmetry with respect to the c axis [$g_{\parallel} = 2.28(1)$; $g_{\perp} = 2.03(1)$] and are almost temperature independent. We compare our results with inelastic neutron scattering and nuclear-magnetic-resonance data.

I. INTRODUCTION

The high- T_c cuprate superconductors are still at the focus of present interest. Despite an enormous amount of experimental and theoretical results the importance of antiferromagnetic (AFM) spin fluctuations for the normal- and superconducting-state properties is still unclear. Focusing on $\text{YBa}_2\text{Cu}_3\text{O}_{6+\delta}$, a universal ω/T scaling of the dynamic susceptibility $\chi''(\omega, T)$ has been detected in the weakly doped metallic state.¹ The same scaling relation has been theoretically proposed by Varma, Littlewood, and Schmitt-Rink² and it was suggested that this non-Fermi-liquid behavior might be related to the unusual normal-state properties. However, it also became clear, that this universal scaling behavior breaks down in more metallic $\text{YBa}_2\text{Cu}_3\text{O}_{6+\delta}$ samples at low energies and for temperatures below 100 K.³

In the superconducting samples a spin pseudogap opens above T_c which appears to be strongly dependent on oxygenation. This has been demonstrated using inelastic neutron scattering^{4,5} (INS) and nuclear-magnetic-resonance (NMR) techniques.⁶ The non-Fermi-liquid behavior of the dynamic susceptibility, namely, that $\chi''(\omega, T)$ decreases with decreasing temperature, has been explained to be due to a singlet pairing of electrons in adjacent CuO_2 planes by Millis and Monien.⁷

In this experimental report we will show that the temperature dependence of the dynamic susceptibility of the CuO_2 planes in $\text{YBa}_2\text{Cu}_3\text{O}_{6+\delta}$ can also be studied by electron-paramagnetic-resonance (EPR) techniques. After the discovery of high- T_c superconductivity by Bednorz and Müller,⁸ the observation of EPR signals in $\text{YBa}_2\text{Cu}_3\text{O}_{6+\delta}$ due to the presence of Cu^{2+} has been reported in a vast amount of literature.⁹ However, soon it became clear that these signals were due to impurity phases¹⁰ or complex paramagnetic defect states.¹¹ Very recently we have demonstrated that intrinsic EPR signals due to the existence of paramagnetic chain fragments

(PCF's) can be detected in $\text{YBa}_2\text{Cu}_3\text{O}_{6+\delta}$ single crystals for concentrations $0.7 \leq \delta \leq 0.9$.¹² Similar results have been obtained earlier by Shaltiel *et al.*,¹³ by Alekseevskii *et al.*,¹⁴ and by Kochelaev *et al.*¹⁵

Here we present a detailed EPR study on $\text{YBa}_2\text{Cu}_3\text{O}_{6+\delta}$ focusing on the temperature dependence of the intensity of the absorption line, as well as on the temperature dependences of the resonance field and the linewidth. The most relevant results can be summarized as follows.

(i) From the temperature dependence of the intensity $I(T)$ we calculated the absolute number of PCF's and we gained information on the static susceptibilities of chains and planes, separately.

(ii) We observed a strong depression of the dynamic susceptibility of the CuO_2 planes, $\chi''(\omega, T)$ at low temperatures which provides experimental evidence for the opening of a spin gap in the heavily doped metallic regime.

(iii) At high temperatures a Korringa-type behavior of the relaxation rate points toward a Fermi-liquid behavior of the spin susceptibility of the planes.

II. EXPERIMENTAL PROCEDURE AND RESULTS

The EPR experiments were performed on almost 30 high-quality single crystals of $\text{YBa}_2\text{Cu}_3\text{O}_{6+\delta}$ ($\sim 1 \times 1 \times 0.1 \text{ mm}^3$) which were kindly provided from three different laboratories (Shubnikov-Institute for Crystallography, Moscow,¹⁶ Institut für Physik der Universität Frankfurt/Main,¹⁷ and Institut für Physikalische Hochtechnologie, Jena¹²). Crystals with small amounts of spurious phases were excluded from further investigations. In the single-phase material the oxygen content was varied by heat treatment in an argon-oxygen atmosphere ($\sim 10 \text{ Pa O}_2$ partial pressure). After the heat treatment the crystals were quenched to liquid-nitrogen temperature.

Nonresonant microwave absorption appearing at the onset of the superconducting state was used to determine T_c of the annealed crystals. The oxygen content δ was determined using the T_c vs δ phase diagram.¹⁸

The EPR measurements were carried out with a Varian E-Line spectrometer at X -band frequency of about 9.3 GHz with 100 kHz field modulation. Temperatures between 4.2 and 300 K were accessible and controlled by an ITC-4 temperature controller in an Oxford Instruments helium-flow cryostat. Considering the orthorhombic crystal symmetry the crystals were mounted on two different sample holders which guaranteed a rotation of the crystal in the external magnetic field with c axis parallel ($\theta=0^\circ$) to perpendicular ($\theta=90^\circ$) or around the c axis ($\theta=90^\circ$).

Well-defined but weak EPR signals were observed in crystals with oxygen concentrations $0.7 \leq \delta \leq 0.9$ and for temperatures $80 < T < 200$ K. A typical example of an experimentally observed spectrum is shown in Fig. 1 for $\text{YBa}_2\text{Cu}_3\text{O}_{6.8}$ ($T_c=63$ K) at 105 K. Here we show the field derivative of the absorption dP/dH vs the magnetic field H for two different angles. Upon rotation of the c axis from parallel ($\theta=0^\circ$) to perpendicular ($\theta=90^\circ$) with respect to the external magnetic field, the resonance field H_{res} is shifted by almost 0.4 kOe. The absorption lines at all angles can be described by Lorentzian line shapes (dashed lines in Fig. 1). A summary of the angle-dependent measurements for $\delta=0.8$ at $T=105$ K is presented in Fig. 2. The angular dependence of the resonance field for $c \parallel H$ to $c \perp H$ is well described by g factors in an $s=\frac{1}{2}$ system with uniaxial symmetry, namely, $g = (g_{\parallel}^2 \cos^2 \theta + g_{\perp}^2 \sin^2 \theta)^{1/2}$ with $g_{\parallel}=2.28(1)$ and $g_{\perp}=2.03(1)$. When the a/b plane is rotated at $\theta=90^\circ$ the resonance field is almost constant for all angles. Similar observations were made in all our specimens.

At this point, the origin of the EPR signal is still unclear. From the angular dependence of the resonance

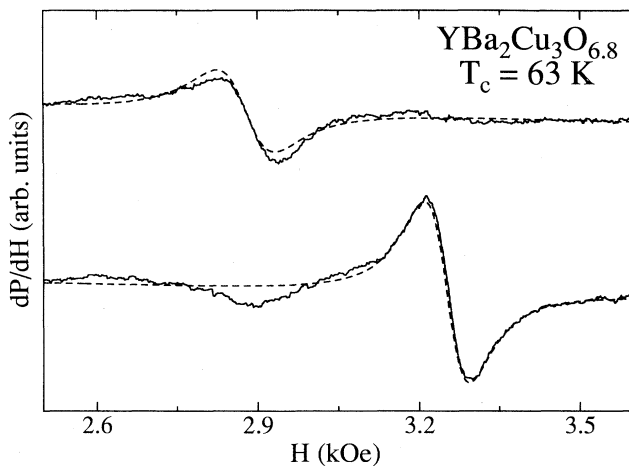


FIG. 1. Absorption derivative dP/dH vs magnetic field H in $\text{YBa}_2\text{Cu}_3\text{O}_{6.8}$ at two different crystal orientations at 105 K. The fits with Lorentzian line shapes are indicated by dashed lines.

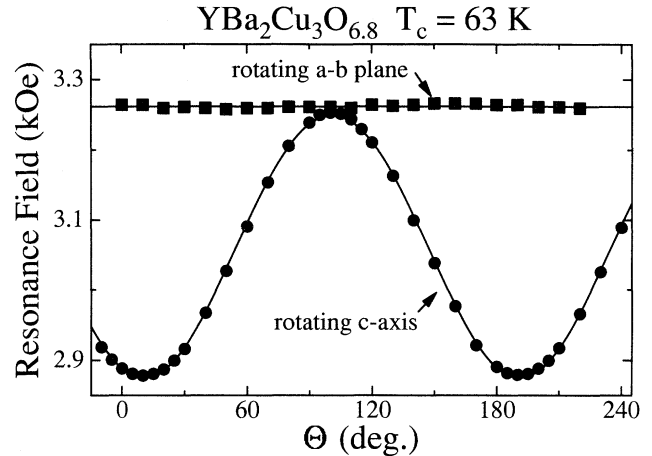


FIG. 2. Angular dependence of the resonance field H_{res} in $\text{YBa}_2\text{Cu}_3\text{O}_{6.8}$ for rotations around two different crystallographic orientations. The results of fits as described in the text are indicated by solid lines.

field, which resembles the symmetry of the crystal, one can conclude that it is an intrinsic paramagnetic center (PC).¹² The observed g values are close to what one expects for Cu^{2+} in a crystal with axial symmetry. But a detailed analysis of the temperature dependences of the intensities of the absorption line, $I(T)$, of the g factors, and of the linewidth of the resonance absorption, $\Delta H(T)$, are needed to gain further insight into the nature of the PC which acts as the EPR probe in $\text{YBa}_2\text{Cu}_3\text{O}_{6+\delta}$. $I(T)$ is determined by the thermal population of the energy levels of the PC in the external field H . For isolated PC's $I(T)$ should follow a Curie behavior. Shifts in the g values are related to the static susceptibilities, while the temperature dependence of ΔH gives insight into the dynamic susceptibility of the CuO_2 planes as seen by the PC's.

The temperature dependences of the intensity of the absorption line, as determined by its area under the absorption curve, of the g factors, and of the linewidth are shown in Figs. 3(a)–3(c). Surprisingly, the intensity of the EPR line reveals only a weak temperature dependence [Fig. 3(a)]. The same is true for the g factors. Both g_{\parallel} and g_{\perp} are almost temperature independent [Fig. 3(b)]. Only at lowest temperature is there a small upturn of both g values. The most interesting and unexpected result was the temperature dependence of the linewidth [Fig. 3(c)]. With decreasing temperatures it decreases, passes through a minimum near 105 K, and steeply increases for further decreasing temperatures. Due to this broadening the absorption line is lost at temperatures approximately 10 K above the superconducting phase transition temperature. Similar observations were made for all single crystals in an oxygen concentration range of $0.7 \leq \delta \leq 0.9$.

Figure 4 shows the dependence of the superconducting phase transition temperature T_c vs the oxygen concentra-

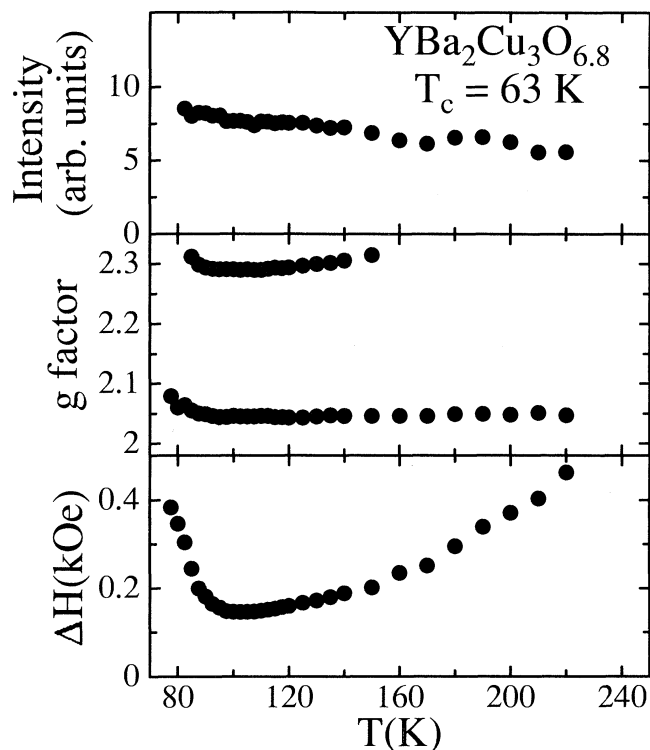


FIG. 3. Temperature dependence of the intensity of the absorption line (a), of the g factors g_{\parallel} and g_{\perp} (b), and of the linewidth (c) in $\text{YBa}_2\text{Cu}_3\text{O}_{6.8}$.

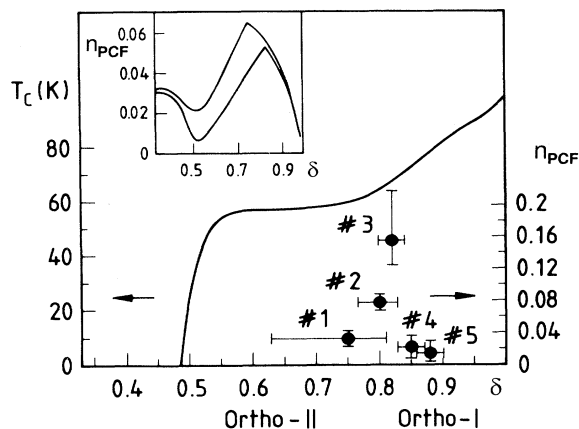


FIG. 4. Oxygen concentration dependence of the fraction of paramagnetic chain fragments n_{PCF} as calculated from the integrated intensity of the EPR signal in $\text{YBa}_2\text{Cu}_3\text{O}_{6+\delta}$ (full symbols, right scale). The concentration dependence of the superconducting phase transition temperature T_c is also shown (solid line, left scale). The inset shows the concentration dependence of paramagnetically active chain fragments for two different "sample preparation" temperatures as calculated using a modified lattice-gas model (see Ref. 19).

tion δ . In this phase diagram we have plotted the observed intensities of the EPR absorption for crystals with different oxygen concentrations at a constant temperature ($T = 105$ K). These intensities are a direct measure of the concentration of PC's in $\text{YBa}_2\text{Cu}_3\text{O}_{6+\delta}$ as a function of δ . EPR signals could be detected for concentrations $0.7 \leq \delta \leq 0.9$ only. No signals were observed for $\delta < 0.7$ and for $\delta > 0.9$.¹² We were able to reproduce the spectra after annealing cycles which first established an oxygen content with $\delta \sim 1$ (no EPR signal) and then decreased δ again into the EPR-active regime. It is interesting to note that the maximum of the EPR absorption is located on the borderline from the orthorhombic phase II to the orthorhombic phase I. It is this regime where PCF's are expected, which are located in the CuO chains.^{12,19} From intensity considerations, in connection with the sensitivity of our spectrometer, it is possible to get a rough estimate of the absolute number of EPR active chain fragments (see Sec. III C). For $\delta = 0.8$ approximately 15% of the Cu ions along the chains contribute to the PCF's. These results can be directly compared to calculations using a modified lattice-gas model¹⁹ (inset in Fig. 4). The theory predicts a maximum of PCF's close to $\delta = 0.8$, exactly where it was detected experimentally. The absolute numbers differ by a factor of 2–3, which is not astonishing considering the experimental uncertainties and the simplified model assumptions.

In the next chapter we will try to analyze the experimental results outlined above. We develop a model in which the PCF's in CuO chains are strongly coupled to the spin system of the CuO_2 planes. Within this model the temperature dependences of the linewidth, the g values, and the intensities can be calculated and compared to the experimental results. Furthermore, this model calculation provides the possibility to gain insight into the spin dynamics of the CuO_2 planes.

III. DISCUSSION AND ANALYSIS

A. Introductory comments

The observed EPR signal has features which can be related to the Cu^{2+} ion having d^9 configuration and the $d_{x^2-y^2}$ orbital as a ground state (axial symmetry, $g_{\parallel} > g_{\perp} > 2$) with z along the c axis of the crystal. One evident candidate for a such a paramagnetic center could be Cu(2) in the middle of a square of O ions in the CuO_2 layer, but it can be ruled out because of an extraordinarily large linewidth due to the anisotropic part of the strong exchange interaction.²⁰ Hence similar signals were usually ascribed to Cu(1) ions in the chains embedded into a specific environment of neighboring oxygen atoms¹⁴ or to paramagnetic chain fragments with oxygen holes.^{14,15} None of the models could consistently describe the observed EPR signals with respect to the electronic structure of Cu(1) ions and the local symmetry of their sites.

For $\delta = 0$ Cu(1) reveals a d^{10} configuration which is not paramagnetic. With increasing doping ($\delta > 0$), for low oxygen content a neutral oxygen atom will accept two electrons from neighboring Cu^+ ions, yielding a Cu^{2+} -

$\text{O}^{2-}\text{-Cu}^{2+}$ configuration. At the same time superexchange interactions will couple the two Cu^{2+} ions to a spin singlet. Each new oxygen atom joining to this shortest fragment of a chain can take now only one electron from the nearest $\text{Cu}(1)$ ion to form Cu^{2+} . In other words, fragments of a chain with n oxygen atoms have $n-1$ holes in the corresponding p^6 configurations and $n+1$ Cu^{2+} ions (one hole in every d^{10} shell). The ground state of this system of $2n$ holes (p and d) will still be a spin singlet state, giving no EPR signal. The appearance of paramagnetically active chain fragments with an odd number of holes (with more than one O^{2-} ion per fragment) can be expected in the region of oxygen doping where the orthorhombic phase II (ortho II) transforms into ortho I. It is interesting that in this transition region from ortho II to ortho I a new superstructure has been detected (ortho III) in which one oxygen-poor chain is followed by two oxygen-rich chains. In the ortho I phase the length distribution of PCF's is similar in all chains, while in the ortho II regime oxygen-poor chains alternate with oxygen-rich ones (Ref. 21, and references therein). According to numerical calculations within an improved lattice-gas model, a sufficient probability to meet such PCF's is found for oxygen concentrations $0.6 < \delta < 0.9$.¹⁹ This is exactly the concentration regime where EPR signals could be observed in our samples. It is worth mentioning that the creation of PCF's is closely related to the transfer of holes into the CuO_2 planes. At the same time this transfer increases the number of O^{2-} ions in the basal planes.

So far, we can understand the existence of EPR signals from CuO PCF's. However, it seems difficult to understand the observed anisotropy of the resonance field by considering the local symmetry of the lattice sites of the PCF's. In the chains Cu^{2+} is located in the center of a slightly distorted square of oxygen atoms $[\text{O}(1), \text{O}(4)]$. Hence approximately the same electronic ground state and the same g factors are expected as those found for the CuO_2 plane, but now with the symmetry axis *parallel* to the plane. However, this is obviously in contradiction with the observed EPR signals. The end of a PCF yields a threefold-coordinated position with no axial symmetry at all, again in contradiction to the experimental results. Our proposal to solve these discrepancies will be given in Sec. III C.

The observed temperature dependence of the EPR linewidth is similar to earlier reports in $\text{YBa}_2\text{Cu}_3\text{O}_{6+\delta}$ single crystals^{13,15} and in $\text{La}_{2-x}\text{Sr}_x\text{CuO}_{4+\delta}$ ceramics doped with Mn (Ref. 22) or Fe.²³ With decreasing temperature the linewidth decreases, passes through a minimum close to 105 K, and strongly increases on further cooling until the signal is lost below 80 K, well above the superconducting phase transition temperature. This behavior is almost opposite to the temperature dependence of the nuclear relaxation rate $1/T_1$ of ^{63}Cu in the high-temperature superconductors.⁶ Nevertheless, there is no doubt that the PCF's have interactions with spin fluctuations of the CuO_2 planes; in particular, there is a superexchange interaction between Cu^{2+} ions belonging to the chain and the plane via the apical oxygen ion $\text{O}(4)$. This interaction gives a contribution to the relaxation

rates, Γ_{cp} , in the same way as for ^{63}Cu nuclear spins in the planes. The corresponding contribution to the EPR linewidth can be written in terms of the imaginary parts of the longitudinal and the transverse dynamical spin susceptibilities $\chi_{\parallel}(\mathbf{q}, \omega)$ and $\chi_{\perp}(\mathbf{q}, \omega)$ of the CuO_2 plane:²⁴

$$\Gamma_{cp} = \frac{k_B T}{(g\mu_B \hbar)^2} J_{cp}^2 \sum_{\mathbf{q}} \text{Im} \left\{ \frac{\chi_{\parallel}(\mathbf{q}, \omega - \omega_s)}{\omega - \omega_s} + \frac{\chi_{\perp}(\mathbf{q}, \omega)}{\omega} \right\}, \quad (1)$$

where J_{cp} is the exchange integral between Cu^{2+} ions located in chains (c) and planes (p) and ω_s is the EPR frequency. The latter is expected to be small in comparison with the important frequencies of AFM fluctuations in the CuO_2 planes.

The nuclear relaxation rate of ^{63}Cu , $1/^{63}T_1$, is given by a similar expression to Eq. (1).⁶ Both quantities, Γ_{cp} and $1/^{63}T_1$, depend on the local dynamic susceptibility but, of course, are characterized by very different coupling mechanisms. Combining the expressions for Γ_{cp} and $1/^{63}T_1$, we can get a rough estimation of Γ_{cp} using the relation

$$\Gamma_{cp} \approx \frac{4}{(g\hbar\gamma)^2} \frac{J_{cp}^2}{A^2} \frac{1}{^{63}T_1}.$$

Here A is the hyperfine coupling constant of the ^{63}Cu nuclear spin. If we take $^{63}T_1 \approx 10^{-3}$ s, $A \approx 50$ kOe/ μ_B ,⁶ and $J_{cp} = 200$ K,²⁵ then we get $\Gamma_{cp} \approx 5 \cdot 10^{12}$ Hz, a value that considerably exceeds the observed EPR linewidth ($\approx 10^8$ Hz). This estimate can be considered as a hint to the existence of a collective motion of magnetic moments of PCF's and CuO_2 planes, making the mutual relaxation unobservable. Theoretical estimates of this so-called bottleneck regime have been given by Barnes²⁶ and Plefka.²⁷ This idea has proven to be helpful also to resolve all the other difficulties mentioned above and will be our starting point for interpretation of the experimental results. As a matter of fact, a similar model of the spin dynamics for PCF's and CuO_2 planes has been used already earlier¹⁴ in order to explain the values of observed g factors and the EPR intensity. Clear evidence of the bottleneck effect²⁶ in the coupled system of the magnetic moments of the EPR probe (here PCF's) and the AFM spin fluctuations in the CuO_2 planes has been demonstrated in EPR measurements of $\text{La}_{2-x}\text{Sr}_x\text{CuO}_{4+\delta}$ doped with Mn.²²

B. Spin dynamics of paramagnetic chain fragments

In addition to the strong spin coupling between PCF's and the spins in CuO_2 planes described above we have to take into account the direct relaxation of the transverse magnetic moments of both spin species to the lattice (1) (in particular, to free carriers in the plane). Both relaxation rates, Γ_{cl} (chain-lattice) and Γ_{pl} (plane-lattice), certainly will contribute to the EPR linewidths. However, if these relaxation rates, Γ_{cl} and Γ_{pl} , are much smaller compared to the relaxation rates between the two spin species, Γ_{cp} , then a single EPR line corresponding to the

collective motion of their transverse magnetic moments will be observed. This situation is similar to the so-called "bottleneck effect" for EPR of localized moments which are coupled to the conduction electrons by the isotropic exchange interaction (see, for example, the review of Barnes²⁶ and the thesis of Plefka²⁷). Explicitly, the condition for the existence of a bottlenecked regime is the following:

$$|\Gamma_{cp} + \Gamma_{pc} + i(\lambda\chi_c\omega_p + \lambda\chi_p\omega_c)| \gg |\Gamma_{pl} - \Gamma_{cl} + i(\omega_p - \omega_c)|. \quad (2)$$

Here ω_c and ω_p are the EPR frequencies of PCF's and the CuO_2 planes; χ_c and χ_p are the corresponding effective spin susceptibilities of chains and planes, including a mutual influence within molecular field theory, and λ is the dimensionless exchange coupling constant between them:

$$\chi_c = \chi_c^0 \frac{1 + \lambda\chi_p^0}{1 - \lambda^2\chi_p^0\chi_c^0}, \quad \chi_p = \chi_p^0 \frac{1 + \lambda\chi_c^0}{1 - \lambda^2\chi_p^0\chi_c^0}, \quad (3a)$$

with

$$\lambda = \frac{4J_{cp}}{N_c g_c g_p \mu_B^2}, \quad \chi_c^0 = n_{\text{PCF}} N_c S(S+1)(g_c \mu_B)^2 \frac{1}{3k_B T}. \quad (3b)$$

We have introduced "bare" magnetic susceptibilities χ_c^0 and χ_p^0 with N_c as the number of Cu ions in chains per cm^3 and n_{PCF} as the concentration of PCF's; g_c and g_p are the corresponding g factors. Differences between the g factors are the reason why the EPR frequencies are involved in Eq. (2), since only the operator of the total spin of PCF's and CuO_2 planes has a zero commutator with the isotropic exchange interaction between them, but not the magnetic moment. Terms with λ in (2) appear due to the additional coupling of the equations of motion for the transverse magnetic moments of these two subsystems, since each of them relaxes to the instantaneous effective alternating field including the corresponding molecular field correction. The relaxation rates Γ_{cp} and Γ_{pc} are connected by the detailed balance equation $g_p^2 \chi_c^0 \Gamma_{cp} = g_c^2 \chi_p^0 \Gamma_{pc}$.

In a phenomenological way, the expected EPR linewidth and g factors in the strong-bottleneck regime can be written immediately in terms of relaxation rates and susceptibilities:²³

$$\frac{g_c \mu_B}{\hbar} \Delta H = \Gamma_{\text{eff}} = \frac{\chi_c^0 \Gamma_{cl} + \chi_p^0 \Gamma_{pl}}{(\chi_c + \chi_p)} + \text{Re} \frac{\langle (\Delta\omega)^2 \rangle}{\Gamma_{cp} + i\lambda\chi_p\omega_c} \quad (4a)$$

and

$$g_{\text{eff}} = \frac{\chi_c g_c + \chi_p g_p}{\chi_c + \chi_p}. \quad (4b)$$

Equation (4) directly shows that the large contributions ($\sim J_{cp}^2$) to the EPR linewidths resulting from Eq. (1) are actually canceled. In addition, the exchange coupling between the two subsystems, PCF's and CuO_2 planes, strongly reduces the possible inhomogeneous broadening

of the EPR line caused by the distribution of local fields, including anisotropic exchange interactions between PCF's, magnetic dipole-dipole interactions, and hyperfine structures. The second term in (4a) represents contributions according to this inhomogeneous broadening; $\langle (\Delta\omega)^2 \rangle$ is the mean square of the bare shift from resonance, producing this inhomogeneous broadening.

According to the model described above, the EPR signal contains information concerning the spin dynamics of both the PCF's and CuO_2 planes. It is evident that this model cannot be fully reduced to the spin dynamics based on the Mila-Rice Hamiltonian²⁸ since the relaxation of the total magnetic moment to the lattice implies the existence of other degrees of freedom, e.g., coupling to holons due to spin-orbit interactions.

C. Data analysis of the EPR absorption line

Intensity of the EPR absorption line

The observed integrated intensity of the EPR absorption line is only weakly dependent on temperature, in clear disagreement with the Curie law which would be expected for PCF's. However, in the model we outlined above the PCF's are strongly coupled to the spins in the CuO_2 planes and both spin species undergo a collective motion of their transverse magnetic moments. In this bottleneck case the intensity of the EPR signal is proportional to the static susceptibilities of chains and planes, i.e., $I \sim \chi_c + \chi_p$. The bare susceptibility χ_p^0 is known from experimentally observed Knight shifts in NMR measurements.⁶ It depends strongly on temperature and continuously increases towards higher temperatures (below 300 K) for metallic samples with $x < 0.94$. Hence we took

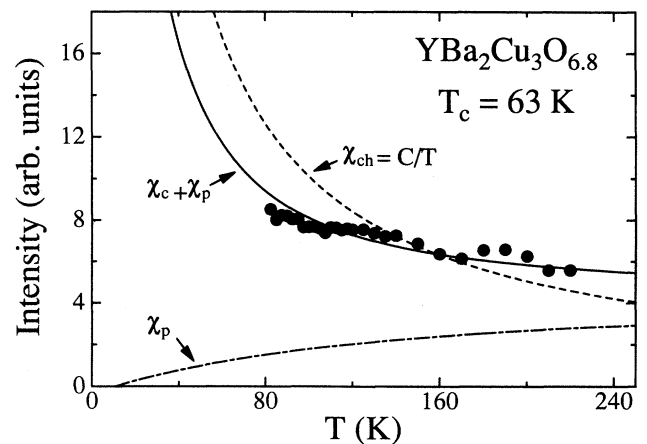


FIG. 5. Temperature dependence of the measured intensities of the EPR absorption lines (solid symbols). The static susceptibility of the CuO_2 planes (χ_p) as determined from the Knight shift in NMR experiments (dashed-dotted line) and the Curie-type susceptibility of the paramagnetic chain fragments (χ_c , dashed line) combine to the total susceptibility which has been fitted to the experimental results (solid line).

the values for χ_p from the Knight-shift data of Ref. 6 and added a Curie law for the chain susceptibility χ_c . The result of this fit using only one single free parameter, namely, the concentration of PCF's, is shown in Fig. 5 for a sample with $\delta=0.8$ ($T_c=63$ K). The agreement with the experimental data is reasonable and similar results were obtained for the other samples investigated. The dependence of n_{PCF} on the oxygen content δ as determined in five different samples is shown in Fig. 4. It reveals a similar concentration dependence as predicted by recent lattice-gas models.¹⁹ However, theoretically the absolute values are overestimated by a factor of 2 to 3 (compare the experimental values as determined in five different crystals with the model calculations shown in the inset of Fig. 4).

g factors

Cu^{2+} ions with a $d_{x^2-y^2}$ ground state reveal a g tensor with axial symmetry and the principal values

$$g_1 = g_2 = 2 + 2u_p, \quad g_3 = 2 + 8u_p, \quad u_p = \lambda/\Delta_p, \quad (5)$$

where λ is the spin-orbit coupling parameter, Δ_p is an averaged crystal-field splitting between the ground state and d_{xy}, d_{xz}, d_{yz} orbitals, and the indices 1, 2, and 3 denote the a , b , and c axes of the orthorhombic unit cell.

In the case of the PCF's the situation is more complicated. The ground state is the superposition of wave functions of d and p orbitals with coefficients which depend on the length of the PCF's. According to the local symmetry of the Cu^{2+} ion in the PCF, the corresponding contribution to the ground state must have the form

$$|d_c\rangle = \cos\frac{\alpha}{2}|d_{x^2-y^2}\rangle + \sin\frac{\alpha}{2}|d_{3z^2-r^2}\rangle \quad (6a)$$

and the corresponding g factors are

$$\begin{aligned} g_1 &= 2 + 2u_c(2 - \cos\alpha - \sqrt{3}\sin\alpha), \\ g_2 &= 2 + 2u_c(2 - \cos\alpha + \sqrt{3}\sin\alpha), \\ g_3 &= 2 + 4u_c(1 + \cos\alpha). \end{aligned} \quad (6b)$$

In twinned single crystals, regions with g_1 and g_2 are interchanged. The contribution of p holes to the ground state should depend on the length of the PCF's, but we expect them to be less important in comparison with Eq. (6a). In the bottleneck regime the effective g factors can then be calculated according to Eq. (4b). In twinned crystals a single EPR line should be observed in directions of the field in between the a and b axis, only

$$g_{\text{eff}}^{\parallel} = \frac{\chi_c \{2 + 4u_c(1 + \cos\alpha)\} + \chi_p(2 + 8u_p)}{\chi_c + \chi_p}, \quad (7a)$$

$$g_{\text{eff}}^{\perp} = \frac{\chi_c \{2 + 2u_c(2 - \cos\alpha)\} + \chi_p(2 + 2u_p)}{\chi_c + \chi_p}. \quad (7b)$$

For other directions in the a, b plane the line should be split. We did not observe two lines, probably owing to the large linewidth. For the Cu^{2+} ion in the fourfold-coordinated position within the chain, on the basis of the

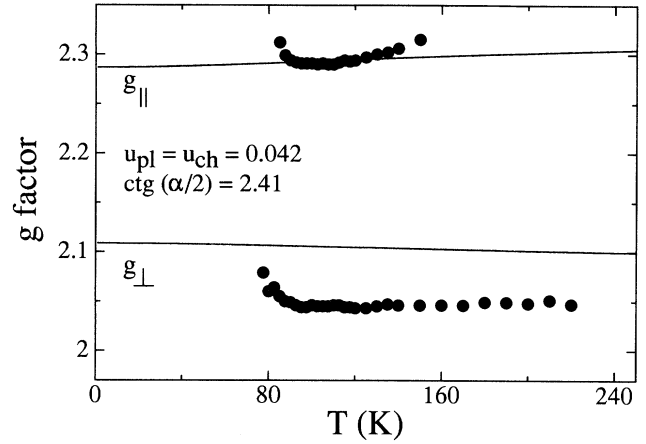


FIG. 6. Temperature dependence of g_{\parallel} and g_{\perp} (solid symbols) compared to the predictions of our model (solid lines).

Knight shift analysis, Mila and Rice suggested the relation $\cot(\alpha/2) = \sqrt{3}$.²⁸ This corresponds to a perfect square of oxygen atoms around the Cu^{2+} ion. However, for PCF's this is not true, especially not for threefold-coordinated Cu ions at the ends of chain fragments. Our attempt to fit the experimental values of g factors using (7a) and (7b) with only one parameter $u = u_c = u_p$ and $\cot(\alpha/2) = 2.41$ is shown in Fig. 6. The absolute values are not well described. This is not astonishing in view of the oversimplified model for the PCF's. But we emphasize that the main features ($g_{\text{eff}}^{\parallel} > g_{\text{eff}}^{\perp}$ and a weak temperature dependence) are correctly reproduced.

Linewidth

Under the assumption that the susceptibilities are known, the temperature dependence of the EPR linewidth, according to Eq. (4a), is determined by the three temperature-dependent functions Γ_{cl} , Γ_{pl} , and Γ_{cp} , and by two constants $\langle(\Delta\omega)^2\rangle$ and λ . To simplify the fitting procedure we used explicitly the assumption $\Gamma_{cl} \ll \Gamma_{pl}$, since the PCF's are not coupled directly to charge carriers. For the relaxation rates of the magnetic moments of the CuO_2 planes to the lattice we assume a Korringa type of behavior, namely,

$$\Gamma_{pl} = bT. \quad (8)$$

This ansatz was successfully used in the case of $\text{La}_{2-x}\text{Sr}_x\text{CuO}_{4+\delta}$ doped with Mn.²² Assuming that in the bottleneck regime the molecular field parameter λ can be neglected, the temperature dependence of the linewidth is essentially determined by the temperature dependence of $F(T) \sim \Gamma_{cp}$, namely,

$$\frac{g_c \mu_B}{\hbar} \Delta H = \Gamma_{\text{eff}} = \frac{\chi_p^0 b T}{(\chi_c^0 + \chi_p^0)} + \frac{A}{F(T)}. \quad (9)$$

Here A and b are temperature-independent fitting param-

eters and $F(T) \sim \Gamma_{cp}$ corresponds to the dynamic susceptibility [see Eq. (1)].

To fit the experimental results of $\Delta H(T)$ it is necessary to develop a model function $F(T)$ for Γ_{cp} , i.e., for the dynamic susceptibility of the planes. According to our discussion in Sec. III A, the relaxation mechanism of PCF's due to spin fluctuations in the CuO_2 planes should be similar to the nuclear relaxation. Hence we have tried to use a function $F(T) \sim 1/T_1(T)$, and $T_1(T)$ taken from NMR measurements.⁶ The result was not satisfying, since it produces an EPR linewidth which increases too slowly for decreasing temperatures. It was also impossible to describe the data using $F(T) \sim T^\alpha$, which was successfully used in the case of $\text{La}_{2-x}\text{Sr}_x\text{CuO}_{4+\delta}$ doped with Mn.²² In this latter case it was assumed that the strong increase of $\Delta H(T)$ towards low temperature is determined by the coupling of the EPR probe to magnon excitations which already exist in the paramagnetic state. Finally, we have chosen a purely phenomenological function for the averaged imaginary part of the dynamic susceptibility, which has been used by Tranquada *et al.*⁵ to explain neutron-scattering results. According to Eq. (1) we took

$$\Gamma_{cp} \sim F(T) = T \left\{ \tanh \left[\frac{\hbar\omega - \hbar\omega_g}{2k_B T} \right] + \tanh \left[\frac{\hbar\omega + \hbar\omega_g}{2k_B T} \right] \right\}, \quad (10)$$

where $\hbar\omega_g$ is an energy which reflects a spin-gap behavior of the dynamic susceptibility. For high temperatures or high measuring frequencies, Eq. (10) yields the ω/T scaling behavior expected for the dynamic susceptibility of the CuO_2 planes.¹

To describe the experimental results of $\Delta H(T)$, A , b , and ω_g in Eqs. (9) and (10) are the only fitting parameters. The result of a fit of Eq. (9) to the temperature dependence of the linewidth in sample 2 is shown in Fig. 7. The agreement between the model and the experimental results is strikingly good. Similar results were obtained for all samples investigated. The relevant fitting parameters were similar for all oxygen concentrations.

The susceptibilities $\chi_c^0(T)$ and $\chi_p^0(T)$ in Eq. (9) have been determined already earlier [Eqs. (3a) and (3b)] to describe the temperature dependence of the intensity of the resonance absorption. However, to describe $\Delta H(T)$ for all oxygen concentrations with a common set of parameters, the fit quality was considerably increased by assuming a concentration of PCF's, \bar{n}_{PCF} , that is constant for all δ , in clear disagreement with the results as shown in Fig. 4. The fact that, on the one hand, $\Delta H(T)$ can be calculated assuming a constant density of PCF's, \bar{n}_{PCF} , but, on the other hand, $I(T)$ which measures the absolute value of PCF's, n_{PCF} , yields a density that strongly depends on δ , can only be explained by assuming an electronic phase separation of the sample.²⁹ EPR results provide evidence that clusters with a high local concentration of PCF's are embedded in a matrix with a low concentration of PCF's. The intensity of the absorption line measures the total number of PCF's. The linewidth

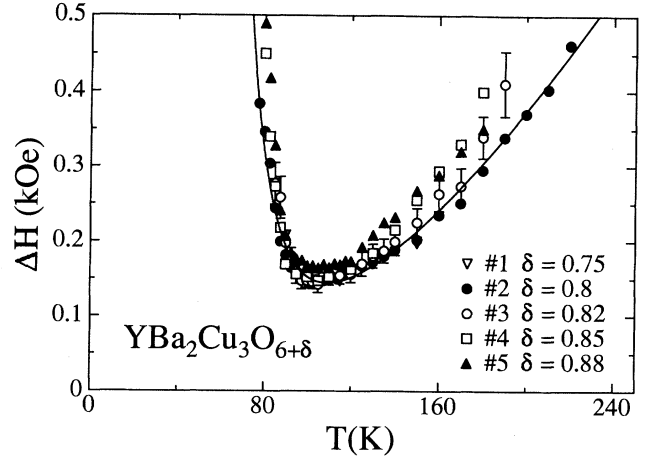


FIG. 7. Temperature dependence of the linewidth ΔH in $\text{YBa}_2\text{Cu}_3\text{O}_{6+\delta}$ for five samples with different oxygen concentrations. The solid line represents the result of a fit using Eq. (9) to the data obtained on sample 2 ($T_c = 63$ K).

is sensitive to the high concentration of PCF's within clusters. Hence $n_{\text{PCF}}(\delta)$ in Fig. 4 describes the δ dependence of the concentration of EPR-active clusters. This electronic phase separation could be enhanced by the quenching procedure we used for the sample preparation and should appear close to the phase boundary of ortho I to ortho II. At the moment, it is unclear if similar explanations would hold assuming a superstructure of oxygen-rich and oxygen-poor chains (i.e., ortho III). Here a more detailed analysis of g values, intensities, and linewidth is needed which, at the moment, is in progress.

The parameters A and b slightly change from sample to sample, but closely match the local concentration of PCF's, \bar{n}_{PCF} . The gap energy $\hbar\omega_g = 45 \pm 10$ meV was kept constant for all oxygen concentrations. The value of the pseudogap resulting from our analysis is almost two times larger than the values resulting from inelastic-neutron-scattering measurements for heavily doped $\text{YBa}_2\text{Cu}_3\text{O}_{6+\delta}$ samples.⁴ However, the values for the spin-gap energy were derived in a very different way, which makes a direct comparison difficult. For example, in the analysis of the gap values from NMR and INS data, only the second term of Eq. (9) has been used, neglecting all other contributions to the temperature dependence of the dynamic structure factor or of the observed relaxation rates. But it is due to the contribution of two temperature-dependent terms in Eq. (9) that our analysis is not very sensitive to the gap value, which results in a relatively large error of $\hbar\omega_g$. However, we can state explicitly that the susceptibility of the planes is drastically suppressed for temperatures below 80 K and at low frequencies. The analysis of INS and NMR data (see Ref. 5) using the phenomenological ansatz of Eq. (10) yielded $\hbar\omega_g = 9$ meV for $\delta = 0.6$ (INS) and $\hbar\omega_g = 18$ meV for $\delta = 0.63$ (NMR).

At the same time we want to point out that, although the general behavior of the EPR linewidth of

$\text{La}_{2-x}\text{Sr}_x\text{CuO}_{4+\delta}$ doped with Mn (Ref. 22) and the system under consideration is very similar, the interpretation is very different. While the broadening of the EPR line with decreasing temperature in the former case could be fitted using Eq. (9) with $F(T) \sim T^\alpha$ and $\alpha \approx 2$, the adequate analysis of the heavily doped $\text{YBa}_2\text{Cu}_3\text{O}_{6+\delta}$ system evidently requires an exponential function displaying pseudogap behavior, consistent with NMR and INS measurements. This interpretation is in accord with the theory of Millis and Monien⁷ who proposed that the decrease of the susceptibility is due to an incipient spin-density-wave ordering in the case of $\text{La}_{2-x}\text{Sr}_x\text{CuO}_{4+\delta}$, but is due to the appearance of a spin gap in $\text{YBa}_2\text{Cu}_3\text{O}_{6+\delta}$.

IV. CONCLUSION

We have presented detailed EPR measurements in $\text{YBa}_2\text{Cu}_3\text{O}_{6+\delta}$ for different oxygen contents. An intrinsic and well-defined signal has been observed only in a narrow concentration range $0.7 < \delta < 0.9$ and can be attributed to the existence of paramagnetic CuO-chain fragments. The weak temperature dependence of the EPR intensity and of the values of the g factors as well as the peculiar temperature dependence of the linewidth can be understood in terms of an isotropic exchange coupling of PCF's to the spin system of the CuO_2 planes, resulting in a collective motion of their magnetic moments (strong-bottleneck regime). Combining a Curie law of the PCF susceptibility with the temperature dependence of the

CuO_2 static susceptibility as determined in NMR measurements, we were able to explain the temperature dependence of the integrated intensity of the EPR absorption line and we were able to estimate the averaged concentration of PCF's as function of the oxygen content δ . The maximum number of PCF's appears close to the phase boundary between ortho II and ortho I phases. These results are qualitatively consistent with theoretical predictions by Uimin and co-workers.^{19,21}

At high temperatures, where the coupling between the two spin systems, namely, the PCF's and the spin fluctuations in the CuO_2 planes, is the strongest, the broadening of the EPR line is caused by the relaxation of the transverse magnetic moment of the CuO_2 planes to the lattice, presumably to the carriers of spin and charge in the same plane. This relaxation rate displays a Korringa-type temperature dependence. At low temperatures the relaxation of PCF's to the spin fluctuations in the CuO_2 planes is dominant. The very steep increase of the linewidth with decreasing temperature can be connected with a pseudogap behavior of the dynamic spin susceptibility of the CuO_2 planes. From the analysis using a phenomenological model we determined the spin gap $\hbar\omega_g = 45 \pm 10$ meV, rather independent of oxygen concentration, in the heavily doped metallic state ($0.75 \leq \delta \leq 0.88$).

ACKNOWLEDGMENT

This research was supported by the Sonderforschungsbereich 252 (Darmstadt/Frankfurt/Mainz/Stuttgart).

*Author to whom correspondence should be addressed. FAX: +49 6151/16-2833.

- ¹R. J. Birgeneau, R. W. Erwin, P. G. Gehring, M. A. Kastner, B. Keimer, M. Sato, S. Shamoto, G. Shirane, and J. Tranquada, *Z. Phys. B* **87**, 15 (1992).
- ²C. M. Varma, P. B. Littlewood, and S. Schmitt-Rink, *Phys. Rev. Lett.* **63**, 1996 (1989).
- ³B. J. Sternlieb, G. Shirane, J. M. Tranquada, M. Sato, and S. Shamoto, *Phys. Rev. B* **47**, 5320 (1993).
- ⁴J. Rossat-Mignod, L. P. Regnault, C. Vettier, P. Burlet, J. Y. Henry, and G. Lapertot, *Physica B* **169**, 58 (1991).
- ⁵J. M. Tranquada, P. M. Gehring, G. Shirane, S. Shamoto, and M. Sato, *Phys. Rev. B* **46**, 5561 (1992).
- ⁶M. Takigawa, A. P. Reyes, P. C. Hammel, J. D. Thompson, R. H. Heffner, Z. Fisk, and K. C. Ott, *Phys. Rev. B* **43**, 247 (1991).
- ⁷A. J. Millis and H. Monien, *Phys. Rev. Lett.* **70**, 2810 (1993).
- ⁸J. G. Bednorz and K. A. Müller, *Z. Phys. B* **64**, 189 (1986).
- ⁹See, e.g., F. Mehran *et al.*, *Phys. Rev. B* **36**, 740 (1987); D. Shaltiel *et al.*, *Solid State Commun.* **63**, 987 (1987).
- ¹⁰See, e.g., G. J. Bowden *et al.*, *J. Phys. C* **20**, L545 (1987); D. C. Vier *et al.*, *Phys. Rev. B* **36**, 8888 (1987); J. Genossar *et al.*, *J. Phys. Condens. Matter* **1**, 9471 (1989); A. Deville *et al.*, *J. Phys. (France)* **50**, 2357 (1989); R. J. Barham and D. C. Doetschman, *J. Mater. Res.* **7**, 565 (1992).
- ¹¹J. Stankowski, W. Hilczek, J. Baszynski, B. Czyzak, and L. Szczepanska, *Solid State Commun.* **77**, 125 (1991).
- ¹²J. Sichelschmidt, B. Elschner, A. Loidl, and K. Fischer, *Z. Phys. B* **93**, 407 (1994).
- ¹³D. Shaltiel, H. Bill, P. Fischer, M. Francois, H. Hagemann,

- M. Peter, Y. Ravi Sekhar, W. Sadowski, H. J. Scheel, G. Triscone, E. Walker, and K. Yvon, *Physica C* **158**, 424 (1989).
- ¹⁴N. E. Alekseevskii, A. V. Mitin, V. I. Nizhankovskii, I. A. Garifullin, N. N. Garifyanov, G. G. Khaliullin, E. P. Khlybov, B. I. Kochelaev, and L. R. Tagirov, *J. Low Temp. Phys.* **77**, 87 (1989).
- ¹⁵B. I. Kochelaev, L. R. Tagirov, I. A. Garifullin, N. N. Garifyanov, G. G. Khaliullin, N. E. Alekseevskii, A. V. Mitin, V. I. Nizhankovskii, and E. P. Khlybov, *Exp. Tech. Phys.* **38**, 359 (1990); I. A. Garifullin, N. N. Garifyanov, N. E. Alekseevskii, and S. F. Kim, *Physica C* **179**, 9 (1991).
- ¹⁶A. B. Bykov, L. N. Demianets, I. P. Zibrov, G. V. Kanunnikov, O. K. Melnikov, and S. M. Stishov, *J. Cryst. Growth* **91**, 302 (1988).
- ¹⁷J. Kowalewski, Ph.D. thesis, University Frankfurt/Main, 1992.
- ¹⁸I. V. Aleksandrov, A. P. Volodin, I. N. Makarenko, L. E. Svislov, and S. M. Stishov, *JETP Lett.* **49**, 327 (1989).
- ¹⁹G. Uimin and J. Rossat-Mignod, *Physica C* **199**, 251 (1992); G. Uimin and V. Stepanov, *Ann. Phys. (Germany)* **2**, 284 (1993).
- ²⁰S. Chakravarty and R. Orbach, *Phys. Rev. Lett.* **64**, 224 (1990).
- ²¹G. Uimin, *Phys. Rev. B* **50**, 9531 (1994).
- ²²B. I. Kochelaev, L. Kan, B. Elschner, and S. Elschner, *Phys. Rev. B* **49**, 13 106 (1994).
- ²³G. Kruschel, Ph.D. thesis, TH Darmstadt, 1993.
- ²⁴M. Coldea, H. Schaeffer, V. Weissenberger, and B. Elschner, *Z. Phys. B* **68**, 25 (1987).
- ²⁵J. Rossat-Mignod, L. P. Regnault, P. Bourges, P. Burlet, C.

- Vettier, and J. Y. Henry, in *Selected Topics in Superconductivity*, edited by L. C. Gupta and M. S. Multani (World Scientific, Singapore, 1993), p. 265.
- ²⁶S. E. Barnes, *Adv. Phys.* **30**, 801 (1981).
- ²⁷T. Plefka, Ph.D. thesis, TH Darmstadt, 1972; *Phys. Status Solidi B* **55**, 129 (1973).
- ²⁸F. Mila and T. M. Rice, *Physica C* **157**, 561 (1989).
- ²⁹A. Furrer, J. Mesot, P. Allenspach, U. Straub, F. Fauth, and M. Guillaume (unpublished).